ACS Photonics

Article

pubs.acs.org/journal/apchd5

Edge States in Dynamical Superlattices

Yiqi Zhang,[*,†,‡] Yaroslav V. Kartashov,[§,⊥,∥] Feng Li,[†] Zhaoyang Zhang,[†,‡] Yanpeng Zhang,[*,†] Milivoj R. Belić,[¶] and Min Xiao[#,△]

[†]Key Laboratory for Physical Electronics and Devices of the Ministry of Education & Shaanxi Key Lab of Information Photonic Technique and [‡]Department of Applied Physics, School of Science, Xi'an Jiaotong University, Xi'an 710049, China

[§]ICFO-Institut de Ciencies Fotoniques, The Barcelona Institute of Science and Technology, 08860 Castelldefels (Barcelona), Spain

[⊥]Institute of Spectroscopy, Russian Academy of Sciences, Troitsk, Moscow Region 142190, Russia

[∥]Department of Physics, University of Bath, Bath BA2 7AY, United Kingdom

[¶]Science Program, Texas A&M University at Qatar, P.O. Box 23874, Doha, Qatar

[#]Department of Physics, University of Arkansas, Fayetteville, Arkansas 72701, United States

[△]National Laboratory of Solid State Microstructures and School of Physics, Nanjing University, Nanjing 210093, China

ABSTRACT: We address edge states and rich localization regimes available in one-dimensional dynamically modulated superlattices, both theoretically and numerically. In contrast to conventional lattices with straight waveguides, not only is the quasi-energy band of an infinite modulated superlattice periodic in the transverse Bloch momentum, but it also changes periodically with an increase in the coupling strength between waveguides. Due to the collapse of quasi-energy bands, dynamical superlattices admit a known dynamical localization effect. If, however, such a lattice is truncated, periodic longitudinal modulation leads to the appearance of specific edge states that exist within certain periodically spaced intervals of coupling constants. We discuss unusual transport properties of such truncated superlattices and illustrate different excitation regimes and enhanced robustness of edge states in them that are associated with the topology of the quasi-energy band.

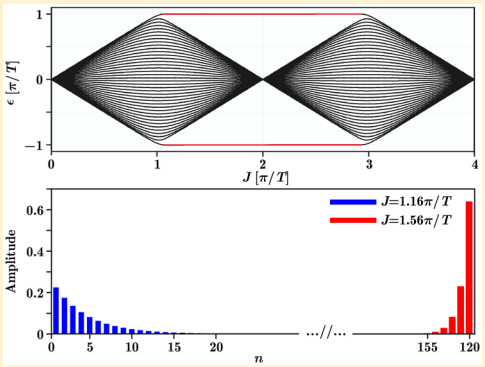

KEYWORDS: *dynamical superlattice, edge states, Floquet evolution operator, quasi-energy, transport property, localization*

Periodically modulated lattice systems attract considerable attention in diverse areas of physics, including condensed matter physics[1−9] and photonics.[10−19] One of the main reasons for the interest in such systems is that due to variations in the parameters of the system along the evolution coordinate (time in condensed matter physis or propagation distance in photonics), not only does a rich variety of resonant dynamical effects associated with specific deformations of quasi-energy bands appear (for an overview of such dynamical effects, see previous literature[20,21]), but one may also encounter the effects of purely topological origin. One of the manifestations of such effects is the appearance of topologically protected edge states that are typically unidirectional (in the 2D systems) and that demonstrate immunity to backscattering on disorder and other structural lattice defects due to topological protection. In modulated periodic photonic systems, frequently called Floquet insulators,[3,15,22] longitudinal variations of the underlying potential were shown to lead to the appearance of the effective external time-dependent "magnetic fields" that qualitatively change the behavior of the system and allow the design of a new class of devices employing topologically protected transport, including photonic interconnects, delay lines, isolators, couplers, and other structures. Periodically modulated photonic lattices were employed for realization of discrete quantum walks[23,24] and allowed observation of Floquet topological transitions with matter waves.[25,26]

Previous investigations of modulated lattices were mainly focused on the 2D and 3D geometries, and less attention was paid to the 1D settings. Moreover, upon consideration of bulk and surface effects in the modulated photonic 1D systems, only simplest lattices were utilized with identical coupling strength between all channels and with identical (usually sinusoidal) laws of their longitudinal variation.[27−33] Only recently dynamical *superlattices* with specially designed periodically varying separation between channels belonging to two different sublattices were introduced that allowed observation of intriguing new resonant phenomena, such as light rectification.[34−36] Previously only bulk modulated superlattices were considered, and no surface effects in such structures were addressed. Therefore, the main aim of this work is the exploration of new phenomena stemming from the interplay between superlattice truncation and its longitudinal modulation. We aim to show that dynamically modulated *truncated* superlattices exhibit topological transition manifested in qualiative modification of the quasi-energy spectrum upon

Received: May 3, 2017
Published: August 17, 2017

DOI: 10.1021/acsphotonics.7b00448
ACS Photonics 2017, 4, 2250−2256

variation of the coupling strength between waveguides forming the lattice. Namely, within proper intervals of coupling strength isolated eigenvalues appear that are associated with nonresonant (i.e., existing within continuous intervals of coupling strengths) edge states. Interestingly, such edge states persist even when conditions for collapse of the bulk quasi-energy band are met. We discuss specific propagation dynamics in the regime, where edge states exist that can be studied in experiments in a conservative and easily realizable system. We believe that these findings substantially enrich the approaches for control of propagation paths of light beams in periodic media.

We also would like to emphasize that the significance of our finding comes from the fact that we use a very simple tight-binding model that is employed for description of excitations in a number of different physical settings, including photonics (with its diversity of fabricated or light-induced guiding structures), matter waves held in the external time-dependent potentials, mechanical anharmonic oscillators, solid-state systems, and biophysics (upon description of energy transport in biomolecules), to name just a few of them. The possibility to implement periodic variations of coefficients (coupling constants) in our physically realizable model introduces a completely unexpected twist to its properties, opening the way to study the whole realm of resonant effects that are not available in similar static structures studied before. Our work deals with one such resonant effect, which was never addressed before, to the best of our knowledge: periodic appearance and destruction of edge states in a truncated superlattice upon variation of coupling strength between waveguides. The predicted effect is universal and purely linear; hence it can be observed in various systems beyond optics.

As an example of the dynamical superlattice we consider the discrete structure depicted in Figure 1, which is somewhat

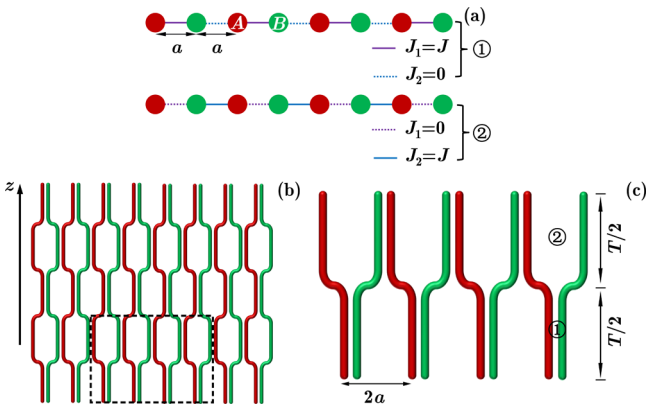

Figure 1. (a) Schematic illustration showing coupling constants on two half-periods of a superlattice composed from sublattices *A* and *B*. Coupling occurs only between sites connected by solid lines and is absent between sites connected by dashed lines. (b) Refractive index distribution in a photonic lattice that reproduces the coupling scheme illustrated in panel (a). (c) Magnification of the region marked by a dashed box in (b) that shows one longitudinal period of the structure.

similar to the Su−Schrieffer−Heeger lattice.[37] The superlattice is composed of two sublattices, denoted as *A* and *B* (red and green channels in Figure 1). The single-mode waveguides in individual sublattices are curved such that the coupling strength between nearest neighbors belonging to different sublattices changes with propagation distance in a step-like fashion, as schematically shown in Figure 1a [since there are two sublattices, one can introduce two coupling strengths $J_1(z)$ and $J_2(z)$ describing coupling between waveguides with equal (n, n) or with different $(n, n+1)$ indices from two sublattices]. We assume that the coupling strength increases to a maximal value J when two waveguides are close and drops down nearly to zero when they are well separated, due to the exponential decrease of the overlap integrals between modal fields with an increase in the distance between the waveguides. The longitudinal period of the structure is given by T, while the transverse period is given by $2a$. In Figure 1c we display one longitudinal period of the structure indicated by a dashed box in Figure 1b. Coupling constants on two different segments of the lattice are indicated in Figure 1a. The lattices considered here can be easily fabricated using a direct femtosecond laser inscription technique.[38] In this technique the ultrashort laser pulses tightly focused inside a sample induce a localized permanent refractive index change in the focal region. When the sample is translated during the writing process, extended waveguide forms. Waveguides can be written along nearly arbitrary longitudinal paths, while sequentially written waveguides can be arranged into large and complex arrays with any geometry (see, e.g., Figure 1), ranging from one- to three-dimensional ones. Typical refractive index distributions created with this technique were discussed previously.[39,40] The refractive index change in each waveguide can be controlled with high precision and is determined by writing speed that can reach 60 mm/min at a pulse energy of 200 nJ and a repetition rate of 100 kHz. This technique has been used for inscription of anomalous two-dimensional topological insulators.[41,42] The dimensionless coupling constant between two single-mode laser-written waveguides m and $m+1$ from Figure 1 is given by $J(z) = (k^2x_0^2/n) \int \delta n_A q_A q_B \, dx / \int q_A^2 \, dx$, where $q_{A,B}(x, z)$ are field distributions in two waveguides $[\max\{q_{A,B}=1\}]$, $\delta n_A(x, z)$ is the small perturbation of the refractive index profile defining the mth waveguide (we assume that it can change with distance), $k = 2\pi n/\lambda$ is the wavenumber, n is the background refractive index, x is the dimensionless transverse coordinate normalized to characteristic scale $x_0 = 10$ μm, and z is the dimensionless propagation distance scaled to diffraction length $kx_0^2 \approx 1.1$ mm. The overlap integral in definition of J depends on the particular shape of the waveguides, and it exponentially decreases with an increase of separation between them (due to exponential localization of the modes). Thus, for two Gaussian waveguides with width 5 μm, 20 μm separation, and refractive index contrast $\delta n_m = 6 \times 10^{-4}$, written in fused silica ($n \approx 1.45$), the coupling constant at wavelength 800 nm is given by $J \approx 0.1$. Complete power transfer between two such waveguides (if they are straight) should occur at a distance $\pi/2J \approx 1.8$ cm, which is substantially smaller than available sample lengths of ~20 cm; that is, many switching events can be observed. By adjusting the separation between waveguides the coupling constant J can be changed by several orders of magnitude and easily reaches the level of $\sim\pi/T$ required for observation of edge states (see below). In the example above with $J \approx 0.1$, such states can be observed in structure with period $T \approx 10\pi$ (i.e., 3.5 cm).

RESULTS AND DISCUSSIONS

Theoretical Model and Band Structure. We describe propagation of light in the infinite superlattice depicted in Figure 1 using the discrete model[43,44]

DOI: 10.1021/acsphotonics.7b00448
ACS Photonics 2017, 4, 2250−2256

$$i\frac{dA_n}{dz} = J_1(z)B_n + J_2(z)B_{n-1}$$
$$i\frac{dB_n}{dz} = J_1(z)A_n + J_2(z)A_{n+1} \quad (1)$$

where coupling constants $J_{1,2}(z)$ are step-like periodic functions of the propagation distance z, while A_n and B_n stand for the field amplitudes on sites of sublattices A and B. According to the Floquet theory, the evolution of excitations in a longitudinally modulated lattice governed by the Hamiltonian $H(\mathbf{k}, t) = H(\mathbf{k}, t + T)$ (here T is the period of longitudinal modulation and $\mathbf{k}$ is the transverse Bloch momentum) can be described by the Floquet evolution operator

$$U(t) = \mathcal{T}\exp[-i\int_0^t H(\mathbf{k}, t')\,dt']$$

where $\mathcal{T}$ is the time-ordering operator. Defining the evolution operator $U(T)$ for one longitudinal period of the structure [i.e., $|\phi(\mathbf{k}, T)\rangle = U(T)|\phi(\mathbf{k},0)\rangle$, where $|\phi(\mathbf{k}, t)\rangle$ is the Floquet eigenstate of the system] and using an adiabatic approximation, one can introduce an effective Hamiltonian H_{eff} of the modulated lattice in accordance with the definition $U(T) = \exp(-iH_{\text{eff}}T)$. In contrast to the instantaneous Hamiltonian $H(\mathbf{k}, t)$, the effective Hamiltonian H_{eff} is z-independent, and it offers a "stroboscopic" description of the propagation dynamics over a complete longitudinal period. The spectrum of the system can be described by quasi-energies ϵ—eigenvalues of the effective Hamiltonian[45,46]—that can be obtained from the expression $U(T)|\phi\rangle = \exp(-i\epsilon T)|\phi\rangle$. Using this approach in the case of an infinite discrete lattice we search for solutions of eq 1 in the form of periodic Bloch waves $A_n = A\exp(ikx_n)$ and $B_n = B\exp(ikx_n + ika)$, where $x_n = 2na$ is the discrete transverse coordinate and $k \in [-\pi/2a, \pi/2a]$ is the Bloch momentum in the first Brillouin zone. Substituting these expressions into eq 1, one obtains

$$i\frac{dA}{dz} = [J_1(z)\exp(iakx) + J_2(z)\exp(-iakx)]B$$
$$i\frac{dB}{dz} = [J_1(z)\exp(-iakx) + J_2(z)\exp(iakx)]A \quad (2)$$

Thus, the Floquet evolution operator over one period can be represented as[2,4,41]

$$U(T) = \exp(-iH_2T/2)\exp(-iH_1T/2)$$
$$= \cos(ak)\exp(-iak) \times \begin{bmatrix} \cos(JT) + i\tan(ak) & i\exp(iak)\sin(JT) \\ i\exp(iak)\sin(JT) & \exp(2iak)[\cos(JT) - i\tan(ak)] \end{bmatrix} \quad (3)$$

where Hamiltonians on the first and second half-periods are given by

$$H_1 = \begin{bmatrix} 0 & J\exp(iak) \\ J\exp(-iak) & 0 \end{bmatrix}$$
$$H_2 = \begin{bmatrix} 0 & J\exp(-iak) \\ J\exp(iak) & 0 \end{bmatrix}$$

One can see from eq 3 that the Floquet evolution operator is a periodic function of transverse momentum k with a period π/a and of the coupling strength J with a period $2\pi/T$. Similarly, by introducing the effective Hamiltonian through $U = \exp(-iH_{\text{eff}}T)$ and calculating its eigenvalues (quasi-energies ϵ), one obtains that the latter are also periodic functions of k and J. In Figure 2, we depict the dependence $\epsilon(k, J)$. The quasi-

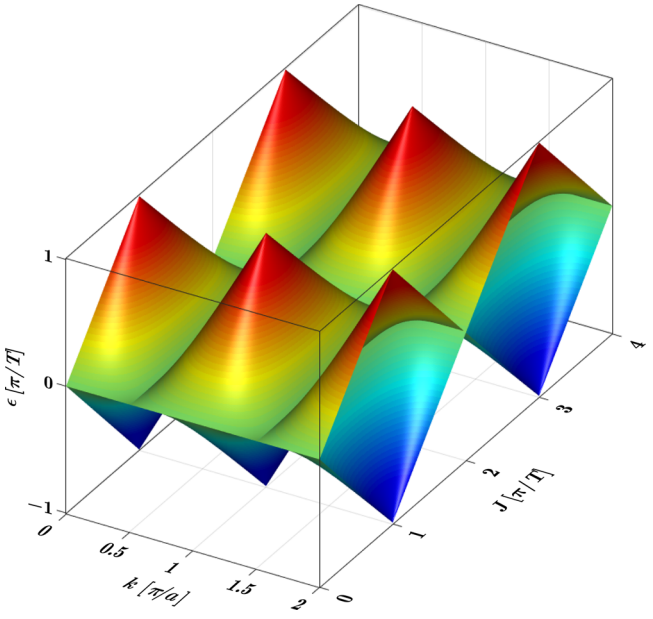

Figure 2. Quasi-energy as a function of Bloch momentum k and coupling constant J.

energy band is symmetric with respect to the plane $\epsilon = 0$ (it is periodic also in the vertical direction with a period $2\pi/T$ because eigenvalues of periodic system are defined modulo $2\pi/T$). The maxima of quasi-energies within a vertical interval shown in Figure 2 are located at $k = n\pi/a$ and $J = (2l + 1)\pi/T$, where n is an integer and l is a non-negative integer. To highlight the details of this dependence we show quasi-energies in Figure 3a and b for certain fixed values of coupling strength J and Bloch momentum k, respectively. Importantly, it follows

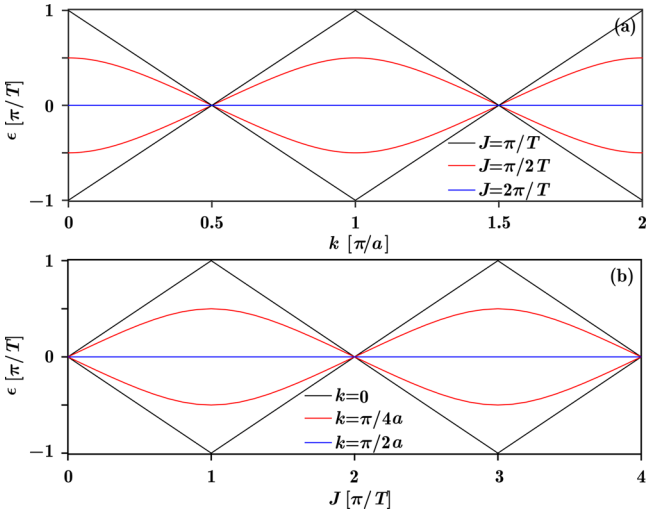

Figure 3. (a) Quasi-energy as a function of k for different J values. (b) Quasi-energy as a function of J for different k values.

DOI: 10.1021/acsphotonics.7b00448
ACS Photonics 2017, 4, 2250−2256

from Figure 3a that the quasi-energy band is dispersive at $J < \pi/T$ (see red curves), so for this coupling strength any localized wavepacket launched into the system will diffract. When J increases up to π/T, the dependence $\epsilon(k)$ becomes linear[47] (see black lines). This means that the effective dispersion coefficient vanishes and excitations in such a lattice will propagate without diffraction, but with nonzero transverse velocity; this is the rectification regime. Further increase of the coupling strength makes the quasi-energy band dispersive again. Finally, the quasi-energy band collapses to a line at $J = 2\pi/T$ (see the blue line). In this regime of dynamical localization the shape of any wavepacket launched into the system will be exactly reproduced after one longitudinal period. Very similar transformations can be observed for different Bloch momenta, when the quasi-energy is plotted as a function of coupling constant J, as shown in Figure 3b.

The situation changes qualitatively when the superlattice is truncated in the transverse direction. In this case one cannot introduce Bloch momentum anymore, so evolution dynamics is described by the system eq 1, where equations for amplitudes in the edge sites A_1 and A_N are replaced by the equations $idA_1/dz = J_1(z)\, B_1$, $idA_N/dz = J_2(z)B_{N-1}$. One should stress that the properties of the system do not change qualitatively if the superlattice is truncated on the site belonging to sublattice A on the left side and on the site belonging to sublattice B on the right side. By introducing an effective Hamiltonian for the finite longitudinally modulated superlattice, one can determine its quasi-energies, which can be plotted as a function of the coupling strength J. In Figure 4a we display the corresponding dependence. One can see that this dependence inherits some features of $\epsilon(J)$ dependence of the infinite lattice (compare Figures 4a and 3b). Among them is the (partial) collapse of the quasi-energy band for specific values of the coupling constant $J = 2\pi m/T$. At the same time, there are two qualitative differences. First, within the interval $J \in [\pi/T, 3\pi/T]$ of coupling constants the isolated quasi-energies emerged (see red lines) that are associated with edge states. In fact, such edge states appear periodically in the intervals $[(4m + 1)\pi/T, (4m + 3)\pi/T]$, where m is an integer. The second difference is that the period of the $\epsilon(J)$ dependence is doubled in comparison with dependence in the infinite lattice. Qualitative modification of the quasi-energy spectrum indicates the topological transition that occurs in the finite modulated superlattice upon variation of the coupling strength between waveguides. Interestingly, the collapse of the quasi-energy band at $J = 2\pi/T$ indicating the presence of dynamic localization in the system coexists with the fact of formation of edge states; so for this particular value of J two qualitative different localization mechanisms are simultaneously available.

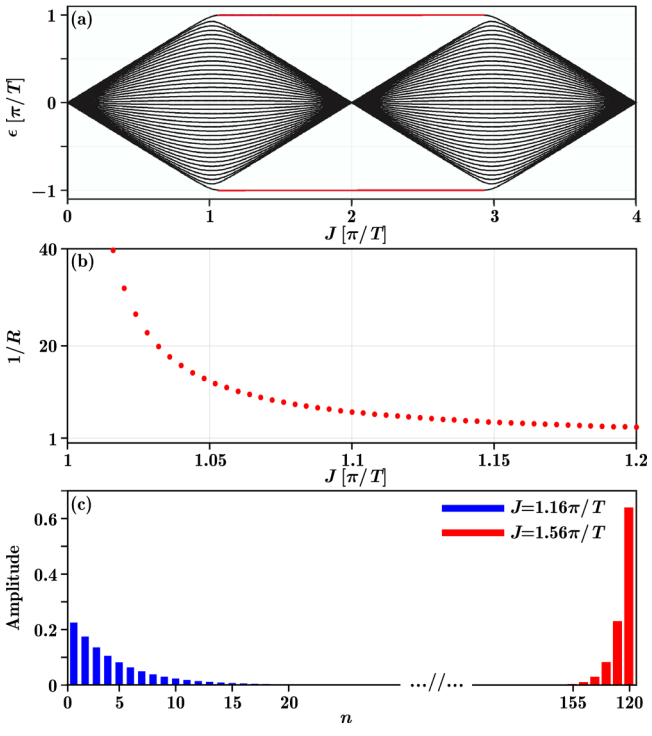

Figure 4. (a) Dependence of quasi-energies on the coupling constant in the finite superlattice containing 200 sites in each sublattice. (b) Width of the edge state versus coupling constant. (c) Absolute value of the edge states corresponding to $J = 1.16\pi/T$ and $J = 1.56\pi/T$, respectively.

The width of the emerging edge states strongly depends on the coupling constant. To illustrate this, we introduce the participation ratio $R = \sum_n |q_n|^4/(\sum_n |q_n|^2)^2$, where $q_n = A_n, B_n$ stands for light amplitudes on sites of sublattices A and B. The width of the mode is inversely proportional to the participation ratio. In Figure 4b, we show the width of the edge state versus coupling constant J. Localization increases with an increase in the coupling constant, so that already at $J > 1.1\pi/T$ the edge state occupies less than 10 sites of the lattice. Maximal localization in a nearly single surface channel occurs at $J = 2\pi/T$, and further increase of the coupling constant leads to gradual delocalization of the edge state. Examples of profiles of edge states (absolute value) with notably different localization degrees at $J = 1.16\pi/T$ and $J = 1.56\pi/T$ are shown in Figure 4c.

Transport Properties. The topological transition that occurs in a finite longitudinally modulated superlattice suggests the existence of novel propagation scenarios in this system. To study transport properties in such structures, we simultaneously consider excitations of the internal and edge sites and use three representative values of the coupling constant. In the particular realization of the lattice that we use to study propagation dynamics (see Figure 5) two edge sites belong to different sublattices; that is, the "bottom" site belongs to sublattice A, while the "top" site belongs to sublattice B. First, we consider the case $J = 0.5\pi/T$, where the quasi-energy band has finite width, while edge states do not appear. In Figure 5a, we excite the internal waveguide and find that the beam diffracts during propagation. Similarly, the excitation of the edge waveguide shown in Figure 5b is also accompanied by rapid diffraction without any signatures of localization. Second, we turn to the system with the coupling strength $J = 1.5\pi/T$. For this coupling constant according to Figure 4a, the width of the quasi-energy band is still finite, but edge states already emerge. Therefore, if an internal site is excited, discrete diffraction will be observed, as shown in Figure 5c. In contrast, excitation of the edge site leads to the formation of a well-localized edge state and only weak radiation can be detected, as shown in Figure 5d. The reason for small radiation is that we use excitation that does not match directly the shape of the edge state; hence delocalized bulk modes are excited too, but with small weights. Finally, we consider the case with $J = 2\pi/T$, where the quasi-energy band collapses (Figure 4a). In this particular case dynamic localization occurs irrespectively of the location of the excited site. In Figure 5e, we show such a localization for excitations of site numbers 10, 20, and 30. In addition, we also excite the edge

DOI: 10.1021/acsphotonics.7b00448
ACS Photonics 2017, 4, 2250−2256

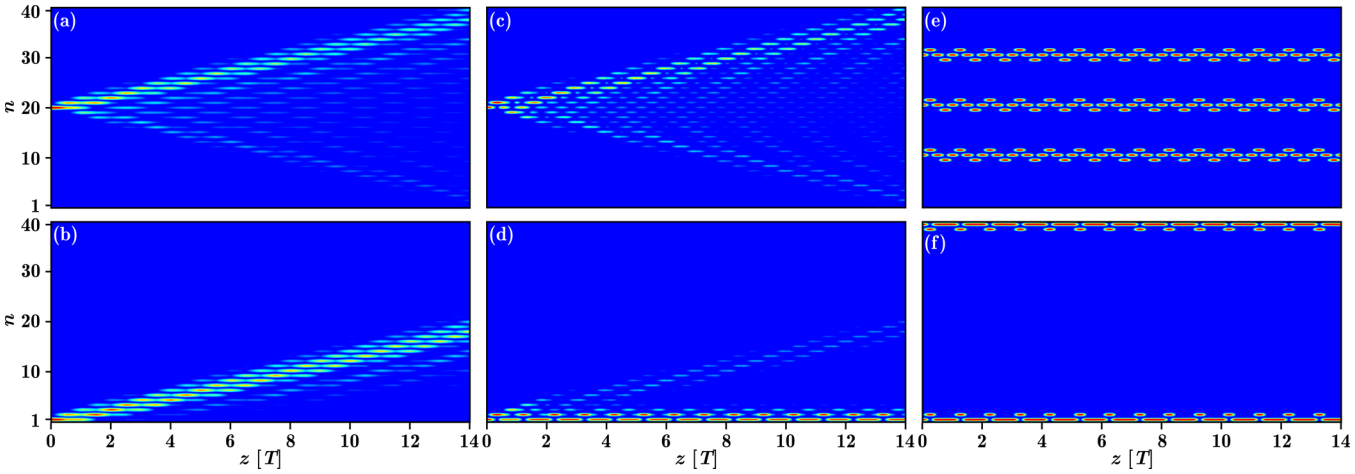

Figure 5. Propagation dynamics in the finite superlattice when only one site in sublattice A is excited by the beam $\exp[-16 \ln 2(x - x_A)^2]$, where x_A is the coordinate of the site in sublattice A. Left panels: Internal site is excited. Right panels: Edge site is excited. First column: $J = 0.5\pi/T$. Second column: $J = 1.5\pi/T$. Third column: $J = 2\pi/T$. Parameters: $a = 1$ and $T = 1$.

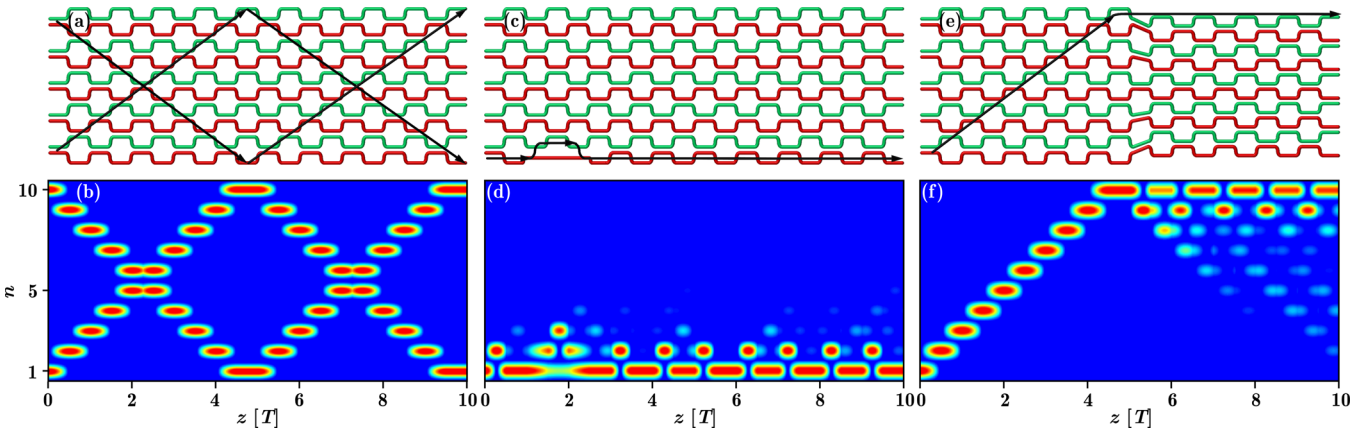

Figure 6. (a) Schematic illustration of the waveguide array without defects or deformation. Black curve with arrows indicates the propagation direction for excitations of two opposite edge waveguides. (b) Propagation dynamics in the lattice without defects at $J = \pi/T$. (c and d) Same as (a) and (b), but for the system with a defect on the edge. For the internal waveguides, the coupling strength is $J = 1.8\pi/T$, while for the straight edge waveguide the coupling strength is $J = \pi/4T$ at $T < z \leq 1.5T$ and $2T < z \leq 2.5T$, and $J = \pi/15T$ at $1.5T < z \leq 2T$. (e and f) Same as (c) and (d), but for the lattice with global deformation that changes the coupling constants after a certain distance z. The coupling strength is $J = \pi/T$ at $0 \leq z < 5T$ and $J = 1.5\pi/T$ at $5T \leq z < 10T$.

waveguides in Figure 5f, where one can see that the light beam does not experience expansion and remains confined in two near-surface sites. This is the regime where two distinct localization mechanisms coexist.

The propagation dynamics in this system is specific at $J = \pi/T$, and it deserves separate discussion. In the infinite lattice this coupling constant corresponds to linear dependence of the quasi-energy on the Bloch momentum k, i.e., the absence of diffraction (rectification regime). The finite superlattice inherits this property to some extent; that is, localized excitations in a finite lattice also do not diffract, but move with constant transverse velocity. Interestingly, despite the absence of diffraction, the excitation of edge states in this regime does not occur, since moving excitations just changes their propagation direction when they hit edge sites. This is illustrated in Figure 6a and b, where we simultaneously excite two opposite edge waveguides. In this particular case we excited sites belonging to different sublattices, as before, but the dynamics does not change qualitatively if sites from one sublattice are excited. Notice that in this interesting regime the transverse confinement occurs without any nonlinearity, and at the same time the propagation trajectory of the beam and its output position can be flexibly controlled, which is advantageous for practical applications. To illustrate enhanced robustness of edge states introduced here, we deliberately introduce considerable deformation at the surface of the lattice, by replacing the whole section of the edge waveguide between $z = T$ and $z = 2.5T$ with a straight section, as shown schematically in Figure 6c. The coupling constant for internal waveguides is selected as $J = 1.8\pi/T$; that is, it corresponds to a situation where edge states form at the surface. The corresponding propagation dynamics in this deformed structure is shown in Figure 6d. Despite considerable deformation of the structure, the edge excitation passes the defect without noticeable scattering into the bulk of the lattice. However, it should be mentioned that if the surface defect is too long and extends over three or more periods of the structure, the edge state may be destroyed and light will penetrate into the depth of the lattice. Finally, we design a structure that is composed of two parts with different coupling strengths between waveguides: in the first part of the lattice $J = \pi/T$ for closely spaced waveguides, while in the second part of the lattice $J = 1.5\pi/T$.

DOI: 10.1021/acsphotonics.7b00448
ACS Photonics 2017, 4, 2250−2256

Such variation in the coupling strength can be achieved by reduction of the transverse period at certain distance z, as shown in Figure 6e. Since in the first part of the lattice the coupling constant is selected such that no edge states can form, but diffractionless propagation is possible, the input beam will propagate from one edge of the lattice toward the opposite edge. If it arrives at the opposite edge in the point, where the coupling constant changes and edge states become possible, the beam may excite the edge state and stay near the surface of the structure, as shown in Figure 6f. If, however, the beam hits the opposite edge before the point where the coupling constant increases, it will be bounced back and enter into the right half of the lattice in one of the internal waveguides. This will lead to fast diffraction of the beam without excitation of the edge states. This setting can be considered as a kind of optical switch, where the presence of signal in the output edge channel depends on the position of the input excitation.

CONCLUSION

Summarizing, we investigated transport properties in the one-dimensional dynamical superlattices. We have shown that in finite modulated superlattices a topological transition may occur that leads to the appearance of edge states, whose degree of localization depends on the coupling constant between lattice sites. This localization mechanism may coexist with dynamic localization due to the collapse of quasi-energy bands. In contrast to systems considered previously, where the entire lattice bends periodically along the evolution coordinate,[28,31] the coupling strength between neighboring channels in our structure is periodically modulated. Due to this modulation, the edge states appear and disappear periodically upon variation of the maximal value of the coupling strength J. We believe that our findings will allow observation of new regimes of dynamical localization of light and provide new insight for topological photonics and quantum-optical analogies.[20,48]

AUTHOR INFORMATION

Corresponding Authors

*E-mail: zhangyiqi@mail.xjtu.edu.cn.
*E-mail: ypzhang@mail.xjtu.edu.cn.

ORCID

Yiqi Zhang: 0000-0002-5715-2182
Yanpeng Zhang: 0000-0002-0954-7681

Notes

The authors declare no competing financial interest.

ACKNOWLEDGMENTS

This work was supported by National Key R&D Program of China (2017YFA0303700), Natural Science Foundation of Shaanxi Province (2017JZ019, 2017JQ6039), China Postdoctoral Science Foundation (2016M600777, 2016M600776), National Natural Science Foundation of China (11474228, 61605154), and Qatar National Research Fund (NPRP 8-028-1-001).

REFERENCES

(1) Oka, T.; Aoki, H. Photovoltaic Hall effect in graphene. *Phys. Rev. B: Condens. Matter Mater. Phys.* **2009**, *79*, 081406.
(2) Kitagawa, T.; Berg, E.; Rudner, M.; Demler, E. Topological characterization of periodically driven quantum systems. *Phys. Rev. B: Condens. Matter Mater. Phys.* **2010**, *82*, 235114.
(3) Lindner, N. H.; Refael, G.; Galitski, V. Floquet topological insulator in semiconductor quantum wells. *Nat. Phys.* **2011**, *7*, 490–495.
(4) Rudner, M. S.; Lindner, N. H.; Berg, E.; Levin, M. Anomalous Edge States and the Bulk-Edge Correspondence for Periodically Driven Two-Dimensional Systems. *Phys. Rev. X* **2013**, *3*, 031005.
(5) Gómez-León, A.; Platero, G. Floquet-Bloch Theory and Topology in Periodically Driven Lattices. *Phys. Rev. Lett.* **2013**, *110*, 200403.
(6) Goldman, N.; Dalibard, J. Periodically Driven Quantum Systems: Effective Hamiltonians and Engineered Gauge Fields. *Phys. Rev. X* **2014**, *4*, 031027.
(7) Asboth, J. K.; Edge, J. M. Edge-state-enhanced transport in a two-dimensional quantum walk. *Phys. Rev. A: At., Mol., Opt. Phys.* **2015**, *91*, 022324.
(8) Xiong, T.-S.; Gong, J.; An, J.-H. Towards large-Chern-number topological phases by periodic quenching. *Phys. Rev. B: Condens. Matter Mater. Phys.* **2016**, *93*, 184306.
(9) Titum, P.; Berg, E.; Rudner, M. S.; Refael, G.; Lindner, N. H. Anomalous Floquet-Anderson Insulator as a Nonadiabatic Quantized Charge Pump. *Phys. Rev. X* **2016**, *6*, 021013.
(10) Yu, Z.; Fan, S. Complete optical isolation created by indirect interband photonic transitions. *Nat. Photonics* **2009**, *3*, 91–94.
(11) Fang, K.; Yu, Z.; Fan, S. Realizing effective magnetic field for photons by controlling the phase of dynamic modulation. *Nat. Photonics* **2012**, *6*, 782–787.
(12) Kitagawa, T.; Broome, M. A.; Fedrizzi, A.; Rudner, M. S.; Berg, E.; Kassal, I.; Aspuru-Guzik, A.; Demler, E.; White, A. G. Observation of topologically protected bound states in photonic quantum walks. *Nat. Commun.* **2012**, *3*, 882.
(13) Khanikaev, A. B.; Mousavi, S. H.; Tse, W.-K.; Kargarian, M.; MacDonald, A. H.; Shvets, G. Photonic topological insulators. *Nat. Mater.* **2012**, *12*, 233–239.
(14) Liang, G. Q.; Chong, Y. D. Optical Resonator Analog of a Two-Dimensional Topological Insulator. *Phys. Rev. Lett.* **2013**, *110*, 203904.
(15) Rechtsman, M. C.; Zeuner, J. M.; Plotnik, Y.; Lumer, Y.; Podolsky, D.; Dreisow, F.; Nolte, S.; Segev, M.; Szameit, A. Photonic Floquet topological insulators. *Nature* **2013**, *496*, 196–200.
(16) Chen, W.-J.; Jiang, S.-J.; Chen, X.-D.; Zhu, B.; Zhou, L.; Dong, J.-W.; Chan, C. T. Experimental realization of photonic topological insulator in a uniaxial metacrystal waveguide. *Nat. Commun.* **2014**, *5*, 5782.
(17) Leykam, D.; Rechtsman, M. C.; Chong, Y. D. Anomalous Topological Phases and Unpaired Dirac Cones in Photonic Floquet Topological Insulators. *Phys. Rev. Lett.* **2016**, *117*, 013902.
(18) Leykam, D.; Chong, Y. D. Edge Solitons in Nonlinear-Photonic Topological Insulators. *Phys. Rev. Lett.* **2016**, *117*, 143901.
(19) Weimann, S.; Kremer, M.; Plotnik, Y.; Lumer, Y.; Nolte, S.; Makris, K. G.; Segev, M.; Rechtsman, M. C.; Szameit, A. Topologically protected bound states in photonic parity-time-symmetric crystals. *Nat. Mater.* **2017**, *16*, 433–438.
(20) Longhi, S. Quantum-optical analogies using photonic structures. *Laser Photonics Rev.* **2009**, *3*, 243–261.
(21) Garanovich, I. L.; Longhi, S.; Sukhorukov, A. A.; Kivshar, Y. S. Light propagation and localization in modulated photonic lattices and waveguides. *Phys. Rep.* **2012**, *518*, 1–79.
(22) Zhang, Y. Q.; Wu, Z. K.; Belić, M. R.; Zheng, H. B.; Wang, Z. G.; Xiao, M.; Zhang, Y. P. Photonic Floquet topological insulators in atomic ensembles. *Laser Photon. Rev.* **2015**, *9*, 331–338.
(23) Broome, M. A.; Fedrizzi, A.; Lanyon, B. P.; Kassal, I.; Aspuru-Guzik, A.; White, A. G. Discrete Single-Photon Quantum Walks with Tunable Decoherence. *Phys. Rev. Lett.* **2010**, *104*, 153602.
(24) Sansoni, L.; Sciarrino, F.; Vallone, G.; Mataloni, P.; Crespi, A.; Ramponi, R.; Osellame, R. Two-Particle Bosonic-Fermionic Quantum Walk via Integrated Photonics. *Phys. Rev. Lett.* **2012**, *108*, 010502.
(25) Asbóth, J. K.; Tarasinski, B.; Delplace, P. Chiral symmetry and bulk-boundary correspondence in periodically driven one-dimensional systems. *Phys. Rev. B: Condens. Matter Mater. Phys.* **2014**, *90*, 125143.

DOI: 10.1021/acsphotonics.7b00448
ACS Photonics 2017, 4, 2250–2256

(26) Dal Lago, V.; Atala, M.; Foa Torres, L. E. F. Floquet topological transitions in a driven one-dimensional topological insulator. *Phys. Rev. A: At., Mol., Opt. Phys.* **2015**, *92*, 023624.
(27) Longhi, S.; Marangoni, M.; Lobino, M.; Ramponi, R.; Laporta, P.; Cianci, E.; Foglietti, V. Observation of Dynamic Localization in Periodically Curved Waveguide Arrays. *Phys. Rev. Lett.* **2006**, *96*, 243901.
(28) Garanovich, I. L.; Sukhorukov, A. A.; Kivshar, Y. S. Defect-Free Surface States in Modulated Photonic Lattices. *Phys. Rev. Lett.* **2008**, *100*, 203904.
(29) Szameit, A.; Garanovich, I. L.; Heinrich, M.; Sukhorukov, A. A.; Dreisow, F.; Pertsch, T.; Nolte, S.; Tünnermann, A.; Kivshar, Y. S. Observation of Defect-Free Surface Modes in Optical Waveguide Arrays. *Phys. Rev. Lett.* **2008**, *101*, 203902.
(30) Longhi, S.; Staliunas, K. Self-collimation and self-imaging effects in modulated waveguide arrays. *Opt. Commun.* **2008**, *281*, 4343−4347.
(31) Szameit, A.; Kartashov, Y. V.; Dreisow, F.; Heinrich, M.; Pertsch, T.; Nolte, S.; Tünnermann, A.; Vysloukh, V. A.; Lederer, F.; Torner, L. Inhibition of Light Tunneling in Waveguide Arrays. *Phys. Rev. Lett.* **2009**, *102*, 153901.
(32) Longhi, S. Dynamic localization and transport in complex crystals. *Phys. Rev. B: Condens. Matter Mater. Phys.* **2009**, *80*, 235102.
(33) Kartashov, Y. V.; Szameit, A.; Vysloukh, V. A.; Torner, L. Light tunneling inhibition and anisotropic diffraction engineering in two-dimensional waveguide arrays. *Opt. Lett.* **2009**, *34*, 2906−2908.
(34) Longhi, S. Rectification of light refraction in curved waveguide arrays. *Opt. Lett.* **2009**, *34*, 458−460.
(35) Dreisow, F.; Kartashov, Y. V.; Heinrich, M.; Vysloukh, V. A.; Tnnermann, A.; Nolte, S.; Torner, L.; Longhi, S.; Szameit, A. Spatial light rectification in an optical waveguide lattice. *EPL (Europhys. Lett.)* **2013**, *101*, 44002.
(36) Kartashov, Y. V.; Vysloukh, V. A.; Konotop, V. V.; Torner, L. Diffraction control in PT-symmetric photonic lattices: From beam rectification to dynamic localization. *Phys. Rev. A: At., Mol., Opt. Phys.* **2016**, *93*, 013841.
(37) Asbóth, J. K.; Oroszlány, L.; Pályi, A. *A Short Course on Topological Insulators: Band Structure and Edge States in One and Two Dimensions*; Springer: Cham, 2016; pp 1−22.
(38) Szameit, A.; Nolte, S. Discrete optics in femtosecond-laser-written photonic structures. *J. Phys. B: At., Mol. Opt. Phys.* **2010**, *43*, 163001.
(39) Blömer, D.; Szameit, A.; Dreisow, F.; Schreiber, T.; Nolte, S.; Tünnermann, A. Nonlinear refractive index of fs-laser-written waveguides in fused silica. *Opt. Express* **2006**, *14*, 2151−2157.
(40) Szameit, A.; Dreisow, F.; Pertsch, T.; Nolte, S.; Tünnermann, A. Control of directional evanescent coupling in fs laser written waveguides. *Opt. Express* **2007**, *15*, 1579−1587.
(41) Maczewsky, L. J.; Zeuner, J. M.; Nolte, S.; Szameit, A. Observation of photonic anomalous Floquet topological insulators. *Nat. Commun.* **2017**, *8*, 13756.
(42) Mukherjee, S.; Spracklen, A.; Valiente, M.; Andersson, E.; Öhberg, P.; Goldman, N.; Thomson, R. R. Experimental observation of anomalous topological edge modes in a slowly driven photonic lattice. *Nat. Commun.* **2017**, *8*, 13918.
(43) Szameit, A.; Rechtsman, M. C.; Bahat-Treidel, O.; Segev, M. PT-formula>-symmetry in honeycomb photonic lattices. *Phys. Rev. A: At., Mol., Opt. Phys.* **2011**, *84*, 021806.
(44) Weimann, S.; Morales-Inostroza, L.; Real, B.; Cantillano, C.; Szameit, A.; Vicencio, R. A. Transport in Sawtooth photonic lattices. *Opt. Lett.* **2016**, *41*, 2414−2417.
(45) Shirley, J. H. Solution of the Schrödinger Equation with a Hamiltonian Periodic in Time. *Phys. Rev.* **1965**, *138*, B979−B987.
(46) Sambe, H. Steady States and Quasienergies of a Quantum-Mechanical System in an Oscillating Field. *Phys. Rev. A: At., Mol., Opt. Phys.* **1973**, *7*, 2203−2213.
(47) della Valle, G.; Longhi, S. Spectral and transport properties of time-periodic PT-symmetric tight-binding lattices. *Phys. Rev. A: At., Mol., Opt. Phys.* **2013**, *87*, 022119.
(48) Gräfe, M.; Heilmann, R.; Lebugle, M.; Guzman-Silva, D.; Perez-Leija, A.; Szameit, A. Integrated photonic quantum walks. *J. Opt.* **2016**, *18*, 103002.

DOI: 10.1021/acsphotonics.7b00448
ACS Photonics 2017, 4, 2250−2256